Preprints of the 21st IFAC World Congress (Virtual)
Berlin, Germany, July 12-17, 2020

RISE Feedback Control of Cable-Driven Parallel Robots: Design and Real-Time Experiments

G. Hassan [*,**] **A. Chemori** [*] **L. Chikh** [***] **P.E. Hervé** [***] **M. El Rafei** [**]
C. Francis [**] **F. Pierrot** [*]

[*] *LIRMM, University of Montpellier, CNRS, Montpellier, France (e-mail: ghina.hassan, ahmed.chemori, francois.pierrot@lirmm.fr)*
[**] *CRSI, Lebanese University, Faculty of Engineering, Beirut, Lebanon (e-mail: maher.elrafei, cfrancis@ul.edu.lb)*
[***] *TECNALIA, Montpellier, France (e-mail: lotfi.chikh, pierre-elie.herve@tecnalia.com)*

Abstract: Control of Cable-Driven Parallel Robots (CDPRs) is considered as a challenging task due to their highly nonlinear dynamic behavior, abundant uncertainties, low-stiff cables, parameters variation, cable tensions, and actuation redundancy. Hence, a robust controller is needed to obtain higher performance despite the above mentioned issues. In this paper, we propose a Robust Integral of the Sign of the Error (RISE) control scheme to solve the problem of reference trajectory tracking. RISE feedback control is a robust nonlinear continuous controller which can guarantee a semi-global asymptotic tracking under limited assumptions on the system's structure. RISE ensures the closed-loop system robustness towards parametric uncertainties and external disturbances. The proposed control solution is designed and implemented in real-time experiments on a fully constrained 4-DOF Cable-Driven Parallel Robot (CDPR) named PICKABLE. The obtained experimental results show that the proposed controller outperforms the classical PID controller and the first-order Sliding Mode Control (SMC) in terms of tracking performances and robustness towards payload variations.

Keywords: RISE control, sliding mode control, PID control, cable-driven parallel robot, real-time experiments.

1. INTRODUCTION

Cable-Driven Parallel Robots (CDPRs) can be defined as a class of traditional parallel robots with the only difference that the elements connecting the mobile platform to the fixed base are flexible cable (Bruckmann and Pott (2012)).
CDPRs have attracted the attention of many researchers in the last decade because they exhibit some interesting properties, compared to rigid-link parallel robots. The total mass and inertia of the moving parts are reduced leading to less energy consumption and high dynamics. CDPRs are capable of handling heavy loads, for example CoGiro CDPR is capable of transporting a payload of 500 Kg (Lamaury and Gouttefarde (2013a)). Moreover, wider workspace can be obtained by CDPRs because the cables can be unwound over great lengths (Baklouti (2018)) (Gouttefarde et al. (2014)). All these advantages make CDPRs well adapted to a very wide range of applications such as handling operations (Pott et al. (2010)), rescue and rehabilitation (Tadokoro et al. (1999)) (Rosati et al. (2007)), pick-and-place (Dallej et al. (2011)), sandblasting and painting (Gouttefarde et al. (2014)).
Like parallel manipulators, the control of a CDPR is considered a challenging task since the nonlinear dynamics and the cables interference increase the complexity of motion control of a CDPR. Besides, CDPRs are known by their abundant uncertainties, singularities, and low-stiff cables. Moreover, Cables can only pull the platform and not push on it. Thus, to ensure the non-negativity of cable tensions an algorithm of Tension Distribution (TD) should be integrated to the control scheme (Lamaury and Gouttefarde (2013b)).
In the literature, we distinguish two main classes of control schemes for CDPRs , namely model-based and non-model-based controllers. The non-model-based control schemes are easy and simple to implement because no dynamic model is required such as the PID controller (Lamaury et al. (2013)) and the robust Lyapunov-based PID controller (Khosravi and Taghirad (2014)). Generally, actuator positions may contain some measurement errors which can degrade the positioning accuracy. To avoid such an issue, (Kino et al. (2007)) has applied a PD controller with adaptive compensation of the actuator position errors. Furthermore, CDPRs inherit nonlinearities from their closed kinematic structure. Hence, the need for model-based controllers clearly arises. A PD control with gravity compensation in joint space was proposed by (Kawamura et al. (2000)). A Nonlinear PD with computed feedforward control has been employed in (Fang et al. (2004)). A computed torque control has been suggested and implemented in (Oh and Agrawal (2005)) and (Williams et al. (2003)). Moreover, (Gholami et al. (2008)) introduced an inverse dynamic control based on a PD feedback strategy in the Cartesian space. To improve the overall tracking performance of a CDPR, a cascade control strategy has been proposed in (Vafaei et al. (2010)). This latter control strategy includes two control loops with two dynamic feedforward terms in both joint and Cartesian spaces. Besides, (Gorman et al. (2001)) proposed a sliding mode control on a cable array robot. This control law shows acceptable accuracy performance, if the robot is needed to be used in an industrial setting. Preliminary investigations in H_∞ control methodology

for CDPRs have been reported in (Laroche et al. (2013)). This methodology allows an improvement of the highest reachable bandwidth.
Despite the simplicity of the latter control schemes, they can not deal with parametric uncertainties and parameter variations of CDPRs. Hence, there is a significant need for model-based adaptive controllers that can compensate the dynamic parameters uncertainties. (Lamaury et al. (2013)) has provided a dual-space adaptive feedforward controller to estimate some dynamic parameters such as friction coefficients and payload mass. Besides, (Gholami et al. (2009)) proposed an adaptive cascade control with gain-adaptation laws to satisfy the desired tracking performance. An adaptive terminal sliding mode control has been designed and applied to a CDPR, named CoGiRo (El-Ghazaly et al. (2015)). In this control law, the dynamics of both the platform and winches were considered and estimated. Although these adaptive model-based control schemes improve the overall performance, they do not take into account external disturbances that can have a significant impact on the tracking error while controlling the CDPR.
The Robust Integral of the Sign of the Error (RISE) feedback control, recently developed in (Xian et al. (2004)), is a good candidate for the control problem of CDPRs. This controller features an integral of the signum function in terms of the combined error ensuring disturbance rejection with a continuous control signal. RISE control technique requires only the position and velocity tracking errors. Moreover, this control law can reduce the chattering effect of the discontinuous signum function by means of the integration. Thanks to their robustness and disturbance rejection ability, RISE and RISE-based control strategies were successfully implemented in different applications such as DC motor drive system (Yao et al. (2014)), nonlinear teleoperation system (Kawai and Namerikawa (2013)) and hard disk drive (Taktak-Meziou et al. (2014). Moreover, they have been validated experimentally on different robotic applications such as underwater vehicles (Fischer et al. (2011)), exoskeleton devices (Sherwani et al. (2019)) and rigid parallel manipulators (Bennehar et al. (2014)) (Saied et al. (2019)).
The aim of this paper is to investigate the ability of RISE control strategy to improve the overall performance of CDPRs in terms of precision and robustness towards parametric uncertainties and external disturbances. The relevance of the proposed RISE controller to a standard PID controller and a first-order sliding mode controller is experimentally validated on a fully constrained 4-DOF CDPR, named PICKABLE. To our best knowledge, RISE controller has never been applied to CDPRs in the literature.
This paper is organized as follows: In Section 2, a brief description of the structure of PICKABLE CDPR is provided, as well as its kinematic and dynamic modeling. The RISE control scheme is presented in Section 3. Section 4 is dedicated to the experimental testbed as well as the presentation and discussion of the obtained experimental results. Section 5, provides conclusions and future work.

2. DESCRIPTION AND MODELING OF PICKABLE CDPR

This section includes a detailed description of PICKABLE robot's structure with its kinematic and dynamic models.

2.1 Description of PICKABLE CDPR

A CAD view of the PICKABLE prototype robot (Yang et al. (2016)) is illustrated in Fig. 1. This prototype is a 4-DOF fully constrained CDPR, developed by Tecnalia within the the European Union project PicknPack. It consists of a fixed-base holding four actuators directly controlling four cables allowing the translation of the platform along the x and y axes as well as its rotation around the z-axis.The mobile platform handles an end-effector for object manipulation purposes.Two additional actuators, integrated to the moving platform, allow the rotation and translation of the end-effector around and along z-axis respectively. This robot is designed to be used in food packaging system in Pick and Place tasks.

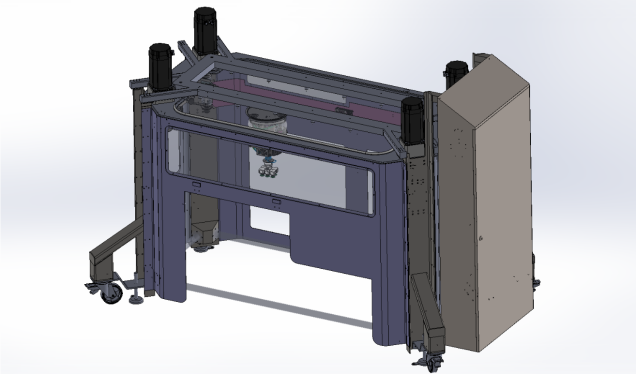

Fig. 1. A CAD view of the PICKABLE CDPR.

The platform has a vacuum chamber allowing it to stick to the ceiling by over-pressure. A docking station was designed to put the platform at rest before and after the task movements. Therefore, once the movement is finished, the over-pressure supplied by the compressor is stopped and the docking station makes it possible to retain the platform.

2.2 Kinematic modeling of PICKABLE CDPR

The general kinematic notations of PICKABLE CDPR are illustrated in Fig. 2. PICKABLE robot has four cable exit points on the fixed-base noted by A_i of position vector a_i, expressed in the robot's fixed reference frame $R_b = \{O, x_b, y_b, z_b\}$, and four cable attachment points on the platform noted by B_i of position vector b_i, expressed in the moving reference frame attached to the platform $R_p = \{P, x_p, y_p, z_p\}$, where $i = 1..4$. The platform Cartesian coordinates are defined by $X = [p^T o^T]^T = [x, y, z, \phi, \theta, \psi]^T \in \mathbb{R}^6$, where the vector p gives the Cartesian position of the geometric center P of the mobile platform and o gives the orientation of the platform with respect to R_b. The orthogonal rotation matrix Q defines the orientation of the moving frame, R_p, with respect to the fixed frame, R_b. In the case of a robot with three DoFs in orientation, the rotation matrix Q is defined as follows:

$$Q(\phi,\theta,\psi) = \begin{bmatrix} c_\theta c_\psi & -c_\theta s_\psi & s_\theta \\ c_\phi s_\psi + s_\phi s_\theta c_\psi & c_\phi c_\psi - s_\phi s_\theta s_\psi & -s_\phi c_\theta \\ s_\phi s_\psi - c_\phi s_\theta c_\psi & s_\phi c_\psi + c_\phi s_\theta s_\psi & c_\phi c_\theta \end{bmatrix}$$

where ϕ, θ, ψ are from the XYZ Euler angle convention. For a simplified representation, $cos(x)$ and $sin(x)$ are denoted respectively by c_x and s_x, $\forall x \in \mathbb{R}$. In the case of PICKABLE CDPR, $\phi = \theta = 0$. The length of the cable i is noted by $l_i \in \mathbb{R}^+$. By noting e_i as a unit vector for the i^{th} cable straight, one can write:

$$\overrightarrow{A_iB_i} = l_i \overrightarrow{e_i}. \quad (1)$$

The Inverse Kinematic Model (IKM) links the platform Cartesian coordinates $X \in \mathbb{R}^6$ to the joint coordinates $l \in \mathbb{R}^4$. To

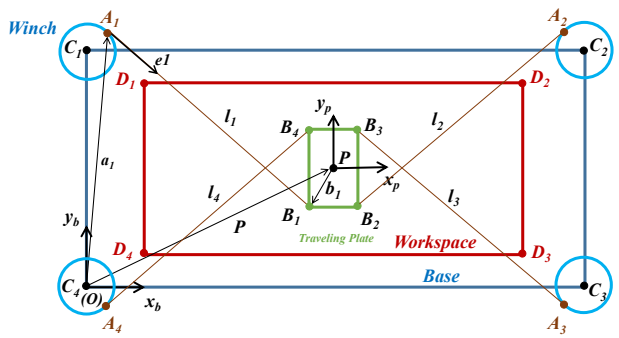

Fig. 2. Illustration through a top view of the kinematics of PICKABLE CDPR.

establish this latter relationship, one can deduce from (1) the geometric constraint of each cable i as follows:

$$l_i = \|p + Qb_i - a_i\|. \tag{2}$$

where $\|.\|$ denotes the Euclidean norm of a vector. The relationship between the i^{th} cable length and the corresponding motor angle can be expressed as follows:

$$l_i = \pm r_i q_i \tag{3}$$

where r_i represents the radius of the i^{th} winch. The first time derivative of (3) yields to a relation between the joint and Cartesian velocities ($\dot{l}$ and $\dot{X}$ respectively), known as the inverse differential kinematic model. It can be expressed as follows:

$$\dot{l} = R\dot{q} = J\dot{X}. \tag{4}$$

where J is the Jacobian matrix of PICKABLE CDPR and R is a diagonal matrix expressed as $R = diag\{r_1, r_2, ..., r_4\}$. The time derivative of (4) yields to the relation between the joint and Cartesian accelerations ($\ddot{l}$ and $\ddot{X}$ respectively) as follows:

$$\ddot{l} = R\ddot{q} = J\ddot{X} + \dot{J}\dot{X}. \tag{5}$$

where $\dot{J}$ is the time derivative of J.

2.3 Dynamic modeling of PICKABLE CDPR

The velocity-force duality of serial and parallel connections of robotic manipulators allows a relation between the vector of cable tensions $t \in \mathbb{R}^4$ and the vector of forces and moments applied to the platform $f \in \mathbb{R}^6$ in the case of CDPRs. This relation can be expressed as follows:

$$f = Wt \tag{6}$$

where $W = -J^T$ is the wrench matrix of a CDPR. The dynamics of a CDPR can be separated into two parts: mobile platform and actuators dynamics (both presented hereafter).

Mobile platform dynamics: The mobile platform dynamics consists of the dynamics of the platform and the payload. Let us assume that the Center of Mass (COM) of the platform, denoted G, coincides with the origin of its frame P. Using the Newton-Euler method (Lamaury et al. (2013)) the mobile platform dynamics can be expressed as follows:

$$M(x)\ddot{x} + C(x,\dot{x})\dot{x} = Wt + f_g(x) \tag{7}$$

where $M(x) \in \mathbb{R}^{6\times6}$ is the mass and inertia matrix, $C(x,\dot{x}) \in \mathbb{R}^{6\times6}$ is the Coriolis and centrifugal matrix.

$$M(x) = \begin{bmatrix} m_t I_3 & 0_{3*3} \\ 0_{3*3} & K \end{bmatrix} \tag{8}$$

$$C(x,\dot{x}) = \begin{bmatrix} 0_{3*3} & 0_{3*3} \\ 0_{3*3} & \dot{K} \end{bmatrix} \tag{9}$$

m_t is the total mass of the platform with payload, $K = QIpQ$ refers to the inertia matrix of the platform expressed at the reference center P, with Ip the inertia matrix of the platform expressed at the COM G. $f_g(x) = [0,0,-m_t g,0,0,0]^T$ represents the gravitational force acting on the platform with its payload. It is worth to note that the platform dynamics equation (7) is only valid for positive cable tensions, $t \geq 0$. Hence, a Tension Distribution (TD) algorithm is required to ensure the positivity of these cable tensions. According to (Lamaury and Gouttefarde (2013b)), a TD algorithm is established by the summation of two terms. The first one is the minimum cable tension solution resulting from the Moore-Penrose generalized inverse of the wrench matrix. While the second one is the homogeneous cable tension solution resulting from the null space of the wrench matrix. Thus, the TD algorithm can be expressed as follows:

$$t_{TD} = W^+ f + (I - W^+ W)t_{Kernel} \tag{10}$$

where t_{Kernel} is a constant arbitrary vector, I is the identity matrix of the appropriate dimension and W^+ the Moore-Penrose generalized inverse of the wrench matrix.

Actuators dynamics: The dynamics of the actuators can be described as follows:

$$\Gamma_m = I_m\ddot{q} + f(\dot{q}) + Rt \tag{11}$$

Where $I_m \in \mathbb{R}^{4\times4}$ is a diagonal matrix representing the moments of inertia of the actuators, $f(\dot{q})$ is the vector of friction torques and Rt is the vector of the torques applied by the cables on the actuators.

Full inverse dynamic model: The inverse dynamic model of the PICKABLE CDPR is obtained by combining (7) and (11) as follows:

$$M(x)\ddot{x} + C(x,\dot{x})\dot{x} - f_g(x) = WR^{-1}[\Gamma_m - (I_m\ddot{q} + f(\dot{q}))] \tag{12}$$

where Γ_m is the vector gathering the actuator torques.

However, some assumptions should be considered to simplify the inverse dynamic model computation. These assumptions can be addressed as follows:
Assumption 1: The gravitational force vector $f_g(x)$ is ignored because it is compensated by the existing air pressure system.
Assumption 2: The Coriolis and centrifugal forces $C(x,\dot{x})\dot{x}$ are neglected.
Assumption 3: The friction force vector $f(\dot{q})$ is neglected
Assumption 4: The cables are assumed to behave as rigid elements neglecting their dynamics.

Therefore, after taking into account the aforementioned assumptions, the inverse dynamic model (12) of PICKABLE CDPR can be rewritten as follows:

$$M(x)\ddot{x} = WR^{-1}[\Gamma_m - (I_m\ddot{q})] \tag{13}$$

with Γ_m being the actuator torques generated by the proposed control scheme.

3. PROPOSED CONTROL SOLUTION: RISE FEEDBACK CONTROLLER

Since CDPRs are often subject to various disturbances and uncertainties, a control law able to take into account these

Fig. 3. View of PICKABLE CDPR prototype.

disturbances and uncertainties is required. RISE feedback control strategy which includes a single integral sign term, can compensate for a large class of uncertainties based on limited assumptions about the disturbance and the controlled system. This continuous feedback control technique produces a semi-global asymptotic tracking despite the presence of unmodeled disturbances and uncertainties in the nonlinear system such as the friction, the interaction with the environment, etc. (Bennehar et al. (2014)).
To achieve the control objective, consider the tracking error e_1 and the combined tracking error e_2 as follows:

$$e_1 = q_d - q \tag{14}$$

$$e_2 = \dot{e}_1 - \alpha_1 e_1. \tag{15}$$

where $q_d \in \mathbb{R}^4$ is the desired position vector of the motor angles, computed from the reference trajectory in the Cartesian space and q is the measured one by means of the actuators encoders. The RISE control law is expressed as follows (Xian et al. (2004)):

$$\begin{aligned}\Gamma_{RISE} &= (K_s+1)e_2(t) - (K_s+1)e_2(t_0) \\ &+ \int_{t_0}^{t} [(K_s+1)\alpha_2 e_2(\sigma) + \beta sgn(e_2(\sigma))]d\sigma.\end{aligned} \tag{16}$$

where $K_s, \alpha_2, \beta \in \mathbb{R}^+$ are positive control design parameters, t_0 is the initial time and $sgn(.)$ is the standard signum function.
In order to control a CDPR using the RISE controller, a TD algorithm should be integrated in the control law. Hence, the actuator input is given by:

$$\Gamma_m = Rt_{TD}. \tag{17}$$

$$t_{TD} = W^+WR^{-1}\Gamma_{RISE} + (1 - W^+W)t_{Kernel} \tag{18}$$

The stability analysis of such controller is established by (Xian et al. (2004)).

4. REAL-TIME EXPERIMENTAL RESULTS

4.1 Experimental testbed of PICKABLE CDPR

The PICKABLE CDPR prototype, illustrated in Fig. 3, has the following main characteristics:

(1) Planar workspace ($X \times Y$): $1200mm \times 400mm$;
(2) The mobile platform has a cubic form with total mass about $8kg$;
(3) The four actuators driving the cables are the B&R 8LSA57.ee022 ETEL direct-drive motors. The maximum provided torque is $69Nm$ and the maximum speed is $9000rpm$;
(4) The two actuators integrated on the platform are the Buehler 1.25.037 brushless motors. Both motors are equipped with an absolute multiturn encoder Heidenhain EBI 1135;
(5) $t_{min} = 0N$ and $t_{max} = 2580N$, where t_{min} and t_{max} are the minimum and the maximum cable tensions respectively. t_{max} is induced by the mechanical design;
(6) The motor rotational positions are measured by means of incremental absolute encoders;
(7) The robot is controlled by a PC equipped with RTX real-time environment where the commands are implemented in C++ with $2kHz$ sampling frequency (i.e. a sample time of $0.5ms$);
(8) The global structure can achieve a peak velocity of $5m/s$, a peak acceleration of $100m/s^2$ and can carry a maximum payload of $2Kg$;

4.2 Experimental results

In order to highlight the performance provided by the RISE control law, a comparison with a PID controller and a first-order SMC is conducted. The PID control law and the SMC law (Perruquetti and Barbot (2002)) in the joint space can be respectively expressed as follows:

$$\begin{aligned}\Gamma_{PID} &= RW^+WR^{-1}(K_p e_1(t) + K_d \dot{e}_1(t) \\ &+ K_i \int_{t_0}^{t} e_1(\tau)d\tau) + R(1 - W^+W)t_{Kernel}.\end{aligned} \tag{19}$$

$$\begin{aligned}\Gamma_{SMC} &= RW^+WR^{-1}(K_1 s + K_2 sgn(s)) \\ &+ R(1 - W^+W)t_{Kernel}.\end{aligned} \tag{20}$$

where K_p, K_d, K_i, K_1 and $K_2 \in \mathbb{R}^{4\times4}$ are diagonal positive definite matrices. s is the sliding surface and is expressed as follows:

$$s = \dot{e}_1 + \alpha_s e_1 \tag{21}$$

where α_s is a positive control design parameter. The feedback gains of the PID, sliding mode and RISE controllers have been tuned by the trial-and-error technique in the conducted real-time experiments and summarized in Table 1.

Table 1. Summary of the feedback control gains.

PID	SMC	RISE
$K_p = 37000$	$K_1 = 85$	$K_s = 85$
Kd = 80	$K_2 = 20$	$\alpha_1 = 600$
Ki = 75	$\alpha_s = 550$	$\alpha_2 = 0.08$
		$\beta = 5$

The Pick-and-Place trajectory illustrated in Fig. 4 is used to evaluate the tracking performance of all the controllers. This reference trajectory is generated in Cartesian space using a 3^{rd} order polynomial S-curve motion profile. The mobile platform starts from the center of the workspace $P0$. It moves to pick up a payload of a mass of $300g$ at point $P1$ at time $t1 = 2s$ with 5% of the maximum velocity and maximum acceleration. The package is then displaced and dropped off at point $P2$ at time $t2 = 6s$. In the last step, the mobile platform returns to the center of the workspace $P0$.
The comparison between the PID, the sliding mode and the RISE controllers in terms of Cartesian tracking errors is depicted in Fig. 5. It is worth to note that the tracking errors of

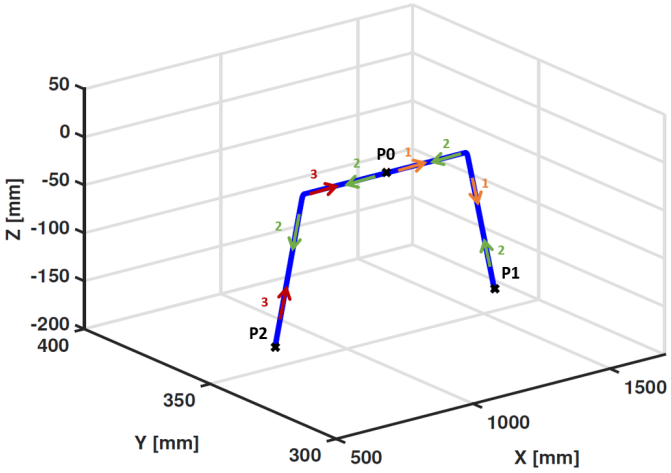

Fig. 4. Pick-and-Place trajectory carrying a mass of 300 g.

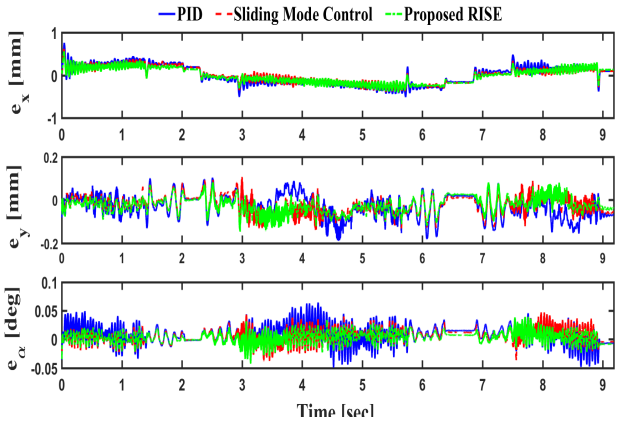

Fig. 5. Evolution of the Cartesian tracking errors versus time.

RISE controller are the smallest, compared to those of PID and sliding mode controllers. The proposed controller significantly outperforms the two other controllers thanks to its capability to compensate the disturbances and the uncertainties, as mentioned previously.

To monitor the performance improvement brought by RISE controller, we consider the Root Mean Square Error of Translation movement (RMSET) and Rotational movement (RMSER) as follows:

$$RMSET = \sqrt{(\frac{1}{N}\sum_{i=1}^{N}(e_x^2(i)+e_y^2(i)))} \tag{22}$$

$$RMSER = \sqrt{(\frac{1}{N}\sum_{i=1}^{N}(e_\alpha^2(i)))} \tag{23}$$

Where e_x, e_y denote the tracking errors along the x and y *axes* respectively, e_α represents the tracking error along the rotational degree of freedom and N is the number of samples. According to the obtained results summarized in Table 2, the translational and rotational tracking errors are reduced by 21% and 42.07% (respectively) with respect of those of PID controller and by 4.3% and 22% (respectively) with respect of those of the sliding mode controller.

The generated control input torques of all controllers are illustrated in Fig. 6. It is clearly observed that all the control signals remain within the admissible limits (i.e. respecting the

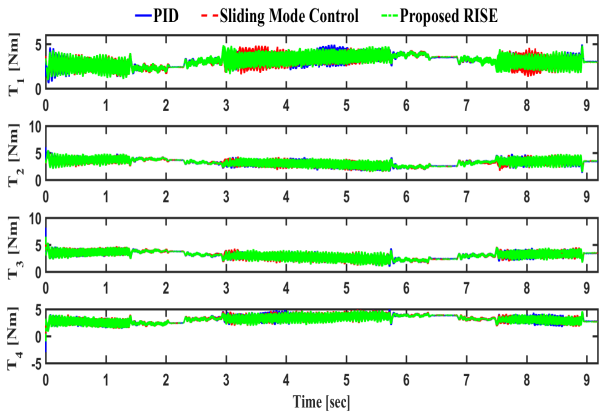

Fig. 6. Evolution of the control input torques versus time.

cables' tensions constraints and the motors saturations). An experimental demonstration of the obtained results can be viewed at the following url: `https://www.youtube.com/watch?v=QCSEr54Czb4`.

5. CONCLUSION AND FUTUR WORK

The main contribution of this paper is a RISE controller applied to redundantly actuated CDPR. The proposed control strategy as well as the standard PID controller and the first-order sliding mode control were implemented in real-time on a 4-DOF CDPR. Experimental results show the superiority of the RISE controller with respect to PID and sliding mode controllers in terms of tracking performance, accuracy and robustness. As a future work, one can consider a more complete dynamic model of the robot, including friction, actuators' dynamics, cables dynamics, etc. to be integrated in the control design.

ACKNOWLEDGEMENTS

This work is supported by Tecnalia "Pick and Throw" research project, the Lebanese University and the social foundation AZM and SAADE.

REFERENCES

Baklouti, S. (2018). *Vibration Analysis and Reduction of Cable-Driven Parallel Robots*. Ph.D. thesis, Rennes, INSA.

Bennehar, M., Chemori, A., and Pierrot, F. (2014). A novel rise-based adaptive feedforward controller for redundantly actuated parallel manipulators. In *2014 IEEE/RSJ International Conference on Intelligent Robots and Systems*, 2389–2394. IEEE, Chicago, USA.

Bruckmann, T. and Pott, A. (2012). *Cable-driven parallel robots*, volume 12. Springer.

Dallej, T., Gouttefarde, M., Andreff, N., Michelin, M., and Martinet, P. (2011). Towards vision-based control of cable-driven parallel robots. In *2011 IEEE/RSJ International*

Table 2. Summary of the tracking performances evaluation.

	PID	SMC	RISE	**Improvements on PID**	**Improvements on SMC**
RMSET mm	0.2296	0.1896	0.1813	**21%**	**4.3%**
RMSER deg	0.0183	0.0136	0.0106	**42.07%**	**22%**

Conference on Intelligent Robots and Systems, 2855–2860. IEEE, San Francisco, USA.

El-Ghazaly, G., Gouttefarde, M., and Creuze, V. (2015). Adaptive terminal sliding mode control of a redundantly-actuated cable-driven parallel manipulator: CoGiro. In *Cable-Driven Parallel Robots*, 179–200. Springer.

Fang, S., Franitza, D., Torlo, M., Bekes, F., and Hiller, M. (2004). Motion control of a tendon-based parallel manipulator using optimal tension distribution. *IEEE/ASME Transactions On Mechatronics*, 9(3), 561–568.

Fischer, N., Bhasin, S., and Dixon, W. (2011). Nonlinear control of an autonomous underwater vehicle: A rise-based approach. In *Proceedings of the 2011 American Control Conference*, 3972–3977. IEEE, San Francisco, USA.

Gholami, P., Aref, M., and Taghirad, H.D. (2009). Adaptive cascade control of the KNTU CDRPM: a cable driven redundant parallel manipulator. In *IEEE International Conference on Robotics and Automation*.

Gholami, P., Aref, M.M., and Taghirad, H.D. (2008). On the control of the KNTU CDRPM: A cable driven redundant parallel manipulator. In *2008 IEEE/RSJ International Conference on Intelligent Robots and Systems*, 2404–2409. IEEE, Nice, France.

Gorman, J.J., Jablokow, K.W., and Cannon, D.J. (2001). The cable array robot: Theory and experiment. In *Proceedings 2001 ICRA. IEEE International Conference on Robotics and Automation (Cat. No. 01CH37164)*, volume 3, 2804–2810. IEEE, Seoul, South Korea.

Gouttefarde, M., Nguyen, D.Q., and Baradat, C. (2014). Kinetostatic analysis of cable-driven parallel robots with consideration of sagging and pulleys. In *Advances in Robot Kinematics*, 213–221. Springer.

Kawai, Y. and Namerikawa, T. (2013). Passivity and rise based robust control for bilateral teleoperation system with communication delay. In *2013 IEEE International Conference on Control Applications (CCA)*, 270–275. IEEE, Hyderabad, India.

Kawamura, S., Kino, H., and Won, C. (2000). High-speed manipulation by using parallel wire-driven robots. *Robotica*, 18(1), 13–21.

Khosravi, M.A. and Taghirad, H.D. (2014). Robust PID control of fully-constrained cable driven parallel robots. *Mechatronics*, 24(2), 87–97.

Kino, H., Yahiro, T., Takemura, F., and Morizono, T. (2007). Robust PD control using adaptive compensation for completely restrained parallel-wire driven robots: Translational systems using the minimum number of wires under zero-gravity condition. *IEEE Transactions on Robotics*, 23(4), 803–812.

Lamaury, J. and Gouttefarde, M. (2013a). Control of a large redundantly actuated cable-suspended parallel robot. In *2013 IEEE International Conference on Robotics and Automation*, 4659–4664. IEEE, Karlsruhe, Germany.

Lamaury, J. and Gouttefarde, M. (2013b). A tension distribution method with improved computational efficiency. In *Cable-driven parallel robots*, 71–85. Springer.

Lamaury, J., Gouttefarde, M., Chemori, A., and Hervé, P.E. (2013). Dual-space adaptive control of redundantly actuated cable-driven parallel robots. In *2013 IEEE/RSJ International Conference on Intelligent Robots and Systems*, 4879–4886. IEEE, Tokyo, Japan.

Laroche, E., Chellal, R., Cuvillon, L., and Gangloff, J. (2013). A preliminary study for H_∞ control of parallel cable-driven manipulators. In *Cable-Driven Parallel Robots*, 353–369. Springer.

Oh, S.R. and Agrawal, S.K. (2005). Cable suspended planar robots with redundant cables: Controllers with positive tensions. *IEEE Transactions on Robotics*, 21(3), 457–465.

Perruquetti, W. and Barbot, J.P. (2002). *Sliding mode control in engineering*. CRC press.

Pott, A., Meyer, C., and Verl, A. (2010). Large-scale assembly of solar power plants with parallel cable robots. In *ISR 2010 (41st International Symposium on Robotics) and ROBOTIK 2010 (6th German Conference on Robotics)*, 1–6. VDE, Munich, Germany.

Rosati, G., Andreolli, M., Biondi, A., and Gallina, P. (2007). Performance of cable suspended robots for upper limb rehabilitation. In *2007 IEEE 10th International Conference on Rehabilitation Robotics*, 385–392. IEEE, Noordwijk, Netherlands.

Saied, H., Chemori, A., Bouri, M., El Rafei, M., Francis, C., and Pierrot, F. (2019). A new time-varying feedback control of PKMs: Theory and application. In *IEEE/RSJ International Conference on Intelligent Robots and Systems*. IEEE, Macau,China.

Sherwani, K.I., Kumar, N., Chemori, A., Khan, M., and Mohammed, S. (2019). Rise-based adaptive control for eicosi exoskeleton to assist knee joint mobility. *Robotics and Autonomous Systems*.

Tadokoro, S., Verhoeven, R., Hiller, M., and Takamori, T. (1999). A portable parallel manipulator for search and rescue at large-scale urban earthquakes and an identification algorithm for the installation in unstructured environments. In *Proceedings 1999 IEEE/RSJ International Conference on Intelligent Robots and Systems. Human and Environment Friendly Robots with High Intelligence and Emotional Quotients (Cat. No. 99CH36289)*, volume 2, 1222–1227. IEEE, Kyongju, South Korea.

Taktak-Meziou, M., Chemori, A., Ghommam, J., and Derbel, N. (2014). A prediction-based optimal gain selection in RISE feedback control for hard disk drive. In *2014 IEEE Conference on Control Applications (CCA)*, 2114–2119. IEEE, Juan Les Antibes, France.

Vafaei, A., Aref, M.M., and Taghirad, H.D. (2010). Integrated controller for an over-constrained cable driven parallel manipulator: KNTU CDRPM. In *2010 IEEE International Conference on Robotics and Automation*, 650–655. IEEE, Anchorage, USA.

Williams, R.L., Gallina, P., and Vadia, J. (2003). Planar translational cable-direct-driven robots. *Journal of Robotic Systems*, 20(3), 107–120.

Xian, B., Dawson, D.M., de Queiroz, M.S., and Chen, J. (2004). A continuous asymptotic tracking control strategy for uncertain nonlinear systems. *IEEE Transactions on Automatic Control*, 49(7), 1206–1211.

Yang, H., Izard, J.B., Baradat, C., Krut, S., Pierrot, F., Gouttefarde, M., and Company, O. (2016). Planar motion device. *EU patent,WO2016096057A1*.

Yao, J., Jiao, Z., and Ma, D. (2014). Rise-based precision motion control of dc motors with continuous friction compensation. *IEEE Transactions on Industrial Electronics*, 61(12), 7067–7075.